

Effect of organophosphate antioxidant on the thermo-oxidative degradation of a mineral oil

Maria Alexandra de Sousa Rios ·
Selma Elaine Mazzetto

Received: 14 November 2011 / Accepted: 13 December 2011 / Published online: 7 January 2012
© Akadémiai Kiadó, Budapest, Hungary 2012

Abstract This study shows the synthesis, characterization, and evaluation of the effect of organophosphate antioxidant on the thermo-oxidative degradation of a mineral oil. The organophosphate was synthesized by nucleophilic substitution (S_N2) of hydrogenated cardanol. For this study, were employed thermogravimetry, derivative thermogravimetry, differential scanning calorimetry, and differential thermal analysis techniques. The results showed that organophosphate contributed for thermo-oxidative stability of mineral oil (initial decomposition temperature (IDT) mineral oil: $91.28\text{ }^\circ\text{C} < \text{IDT mineral oil} + \text{organophosphate (1\%): } 156.42\text{ }^\circ\text{C}$). The organophosphate obtained shows significant thermal stability when compared with other compound of the same class (diphenyl phosphate).

Keywords Cashew nut shell liquid · Alkylphenol · Diphenyl phosphate

Introduction

Oxidative degradation is a common problem in several industrial processes, especially those involving hydrocarbon

materials such as oils, fuels, biofuels, and polymers [1–4]. In particular, when an automotive lubricant or a lubricant for any mechanical system is being used, this oxidizes more quickly, depending on its type (paraffinic, naphthenic, or aromatic), operational conditions, environmental, and other parameters [5, 6]. Therefore, the study of the thermo-oxidation mechanism of this product can help find means of overcoming this disadvantage [7].

According to the literature [8–10], oxidation is a complex chemical reaction and the hydrocarbon degradation process can be divided into three phases: an initial oxidative phase, a medium oxidative phase, and a deep oxidative phase [7]. In a naphthenic lubricant oil, saturated hydrocarbons account for more than 95% of its composition. Therefore, in the oxidative phases, this oil will yield many products of oxidation such as carbonyl compounds, peroxy and hydroxyl radicals, hydroperoxides, and others [7, 11–13].

For this reason, the oxidation of the lubricant is undesirable because in certain cases it can increase lubricant viscosity; hence its ability to be pumped to parts needing lubrication. In this context, a good thermo-oxidative stability is important so that the lubricant does not lose its integrity or form corrosive products and deposits during service, or both [7]. Among several possibilities to reduce and or prevent the speed of the oxidation reactions, chemical industries have been adding antioxidants in their formulations to improve the oxidative stability of these lubricant oils.

Antioxidants are organic compounds that are added to oxidizable organic materials to retard oxidation and, in general, to prolong the useful life of the substrates [14–17]. These additives are classified as either radical trapping (chain breaking) or peroxide decomposing, terms that describe the mechanisms by which they function. The radical trapping antioxidants such as hindered phenols and

M. A. de Sousa Rios (✉)
Departamento de Química – Grupo de Inovações Tecnológicas e Especialidades Químicas - GRINTEQUI, Universidade Federal do Piauí, Campus Ministro Petrônio Portella, Teresina, PI CEP 64.049-550, Brazil
e-mail: maria.alexandra@terra.com.br

S. E. Mazzetto
Departamento de Química Orgânica e Inorgânica – Laboratório de Produtos e Tecnologia em Processos - LPT, Universidade Federal do Ceará, Campus do Pici, Bloco 935, Fortaleza, CE CEP 60.455-760, Brazil

secondary aromatic amines react with oxygen radicals (peroxy and alkoxy), while phosphites and phosphates function as peroxide decomposing by abstracting peroxidic oxygen from hydroperoxides and peroxides, and reducing them [11, 12, 18].

Among the peroxide decomposing antioxidants, the organophosphate is one of the most important types of compound of this class. Thus, this study involved the synthesis, characterization, and investigation of the antioxidant potentiality of an organophosphate derived from cashew nut shell liquid (CNSL) when added to mineral oil. CNSL is constituted of anacardic acid, cardanol, and cardols which are alkyl-substituted phenolic compounds (Fig. 1) [19–22].

For the characterization of the new molecule, the authors used ^1H , ^{13}C , ^{31}P RMN, GC–MS, and its stability, and antioxidant potentiality was evaluated using thermogravimetric analyses (TG–DTG, DSC, and DTA). Thermal parameters such as number of degradation steps, onset (T_{onset}) and maximum (T_{max}) degradation temperatures, percentage of loss of mass (Δm (%)), initial decomposition temperature (IDT), and the integral procedure decomposition temperature (IPDT) [23] were determined in this study.

Materials and methods

Materials

Cashew nut shell liquid and hydrogenated cardanol were supplied by Laboratório de Produtos e Tecnologia em Processos, Brazil. The hydrogenated cardanol was purified by column chromatography on silica gel using hexane as eluent [12]. The alkylphenol was synthesized by alkylation

of hydrogenated cardanol with *tert*-amyl chloride in the presence of Lewis acid (zinc chloride) [14, 24], and the organophosphate was obtained by nucleophilic substitution ($\text{S}_{\text{N}}2$) with diethyl chlorophosphate (DECP). The lubricant oil was supplied by Petrobras (Brazilian Oil Company, Brazil) with no further distilled procedure. The reagents and solvents were supplied by Aldrich (analytical grade).

Physical measurements

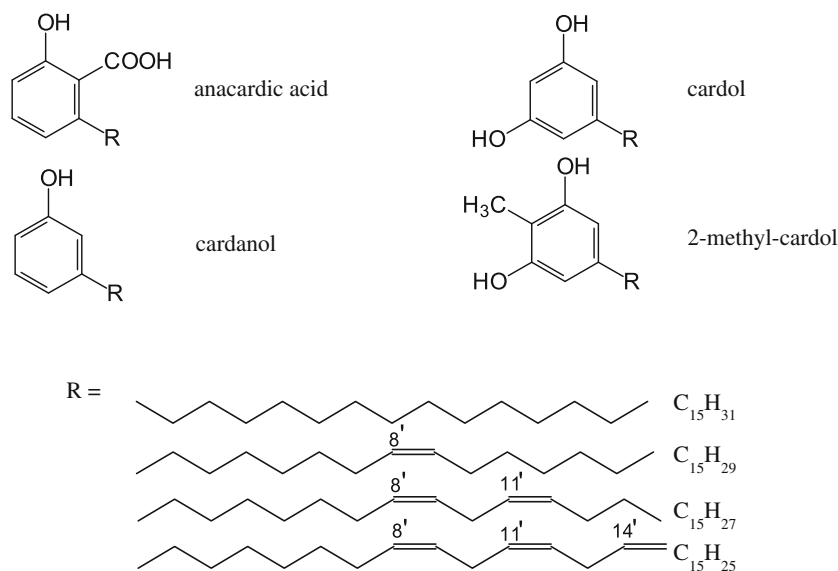
NMR (^1H , ^{13}C , and ^{31}P) spectra were recorded by AVANCE DRX 500 BRUKER spectrometer, at a frequency of 500 MHz under the following conditions: solvent, CDCl_3 ; tetramethylsilane (TMS) as an internal standard for ^1H and ^{13}C , and phosphoric acid (H_3PO_4) for ^{31}P .

GC–MS analyses were performed by the use of Hewlett-Packard 5890 gas-chromatograph and by a Hewlett-Packard 5971A spectrometer equipped with a DB-5 column (0.25 mm, 30 m, 0.25 μm film) used an oven temperature program that initiated data collection at a temperature of 100 $^\circ\text{C}$ and ramped at 10 $^\circ\text{C min}^{-1}$ to 300 $^\circ\text{C}$, holding this temperature for the remaining duration of the data collection. Electron impact (EI, 70 eV) mode was used. Sample of 1 μL was injected into the column.

IR spectra were obtained by the use of a FT-IR spectrophotometer Shimadzu, model 8300 (KBr window).

Thermoanalytical measurements were obtained in a SHIMADZU TGA-50H thermobalance, using alumina pans and a heating rate of 10 $^\circ\text{C min}^{-1}$, in the temperature range 25–900 $^\circ\text{C}$ and samples of approximately 10 mg. The samples were carried out in nitrogen and synthetic air atmospheres (50 mL min^{-1}). The DSC curve was obtained with a SHIMADZU DSC-50 differential scanning calorimeter in the temperature range 25–500 $^\circ\text{C}$, using

Fig. 1 Chemical structures of CNSL constituents



aluminum pans, at a heating rate of $10\text{ }^{\circ}\text{C min}^{-1}$ and samples of approximately 10 mg. A nitrogen atmosphere was used at a flow rate of 50 mL min^{-1} . The differential thermal analysis (DTA) curves were obtained with a SHIMADZU DTA-50H DTA in the temperature range $25\text{--}900\text{ }^{\circ}\text{C}$, using platinum pans, at a heating rate of $10\text{ }^{\circ}\text{C/min}$ and samples of approximately 10 mg. Synthetic air atmosphere was used at a flow rate of 50 mL min^{-1} .

Methods

Synthesis of alkylphenol

The alkylphenol was synthesized by alkylation of hydrogenated cardanol (3.3 mmol) with *tert*-amyl chloride (3.4 mmol) in the presence of Lewis acid (zinc chloride). The reagents were dissolved in chloroform (20 mL), and the mixture was heated under reflux during 4 h until the reaction was completed (monitored by thin-layer chromatography). After 4 h, when no more significant changes in the reaction were observed, the mixture was poured into a separatory funnel, washed with 5% aqueous sodium bicarbonate and then with water. The organic phase was separated, dried with anhydrous sodium sulfate, and evaporated under reduced pressure. A yield of 82% was reached, and the product was purified through a silica gel chromatographic column using solution of hexane/chloroform (80:20). The product was characterized using ^1H NMR and IR [14, 25].

Synthesis of organophosphate

The organophosphate was synthesized by nucleophilic substitution ($\text{S}_{\text{N}}2$). The stoichiometry ratio of the reaction system was of 1.0 mol of alkylphenol:1.0 mol of sodium hydroxide:1.0 mol of DECP, respectively. The reagents were dissolved in chloroform (20 mL), and the mixture was heated under the reflux system with constant agitation at $60\text{ }^{\circ}\text{C} (\pm 1\text{ }^{\circ}\text{C})$ for 1 h and 35 min. After the reaction time, a viscous yellow oil was obtained [12, 18]. A yield of 74% was reached, and the product was purified through a silica gel chromatographic column using solution of hexane/chloroform (70:30). The product was characterized using ^1H , ^{13}C , ^{31}P NMR, GC-MS, TG-DTG, and DSC [26].

Results and discussion

^1H NMR and IR-alkylphenol

Physical state and color: yellow oil. The analysis by ^1H NMR showed the following (CDCl_3 , ppm): 0.98 (3H, triplet, $-\text{CH}_2-(\text{CH}_2)_{12}-\underline{\text{CH}}_3$); 1.32 (24H, multiplet,

$-(\underline{\text{CH}}_2)_{12}-$); 1.45 (6H, singlet, $-(\text{CH}_3)(\text{CH}_2)(\underline{\text{CH}}_3)_2$); 2.60 (2H, triplet, $-\underline{\text{CH}}_2-\text{Ar}$); 6.53 (1H, sharp singlet, $\text{Ar}-\underline{\text{OH}}$); 6.77–7.26 (aromatic protons signals). IR (ν , KBr, cm^{-1}): 3,364 (OH, hydroxyl group of phenol); 2,929 ($\nu_{\text{as}}\text{CH}_2$, asymmetrical stretching); and 2,854 ($\nu_{\text{s}}\text{CH}_2$, symmetrical stretching) methylene groups; 1,625 and 1,576 (C=C ring stretch); 983, 818, 723 (angular C–H deformation of the aromatic ring).

^1H , ^{13}C , ^{31}P NMR, GC-MS, TG-DTG, and DSC-organophosphate

Physical state and color: viscous yellow oil. The analysis by ^1H NMR showed the following (Acetone- d_6 , ppm): 0.64 (3H, triplet, $\underline{\text{H}}_3\text{CCH}_2(\text{CH}_3)_2\text{C}-$); 0.88 (3H, triplet, $-\text{CH}_2-(\text{CH}_2)_{12}-\underline{\text{CH}}_3$); 1.30 (6H, triplet, $(-\text{O}-\text{CH}_2\underline{\text{CH}}_3)_2$); 1.34 (24H, multiplet, $-(\underline{\text{CH}}_2)_{12}-$); 1.38 (6H, singlet, $-(\underline{\text{CH}}_3)_2$); 2.58 (2H, triplet, $-\underline{\text{CH}}_2-\text{Ar}$); 4.22 (4H, quintet, $(-\text{O}-\underline{\text{CH}}_2\text{CH}_3)_2$); 6.94 (1H, duplet, $\text{Ar}-\underline{\text{H}}$); 7.19 (1H, duplet $\text{Ar}-\underline{\text{H}}$); 7.21 (1H, duplet $\text{Ar}-\underline{\text{H}}$); 7.33 (1H, singlet, $\text{Ar}-\underline{\text{H}}$).

$^{13}\text{C}\{^1\text{H}\}$ NMR, showed the following (Acetone- d_6 , ppm): 14.98 (1C, $-\text{CH}_2-(\text{CH}_2)_{12}-\underline{\text{CH}}_3$); 17.07 (2C, $(-\text{O}-\text{CH}_2\underline{\text{CH}}_3)_2$); 34.90 (1C, $\text{H}_3\text{CCH}_2(\underline{\text{CH}}_3)_2\text{C}$); 39.26 (1C, $\text{H}_3\text{CCH}_2(\text{CH}_3)_2\underline{\text{C}}$); 65.43 (2C, $(-\text{O}-\underline{\text{CH}}_2\text{CH}_3)_2$); 120.62 (1C, $\text{Ar}-\underline{\text{C}}_3$), 125.44 (1C, $\text{Ar}-\underline{\text{C}}_4$), 129.88 (1C, $\text{Ar}-\underline{\text{C}}_6$), 136.00 (1C, $\text{Ar}-\underline{\text{C}}_5$), 143.40 (1C, $\text{Ar}-\underline{\text{C}}_2$), 151.50 (1C, $\text{Ar}-\underline{\text{C}}_1$), in accordance with the literature data [12, 25, 27]. $^{31}\text{P}\{^1\text{H}\}$ NMR (Acetone- d_6 , ppm): -5.58 (1P, singlet, $\text{O}=\underline{\text{P}}-(\text{OC}_2\text{H}_5)_2$), in accordance with the literature data [25, 27].

GC-MS analysis showed the molecular ion at m/z 510 (5, $[\text{M}^+ = \text{C}_{30}\text{H}_{55}\text{O}_4\text{P}^+]$), 482 (100, $\text{C}_{28}\text{H}_{51}\text{O}_4\text{P}^+$), 453 (10, $\text{C}_{26}\text{H}_{46}\text{O}_4\text{P}^+$), 425 (12, $\text{C}_{24}\text{H}_{42}\text{O}_4\text{P}^+$), 201 (8, $\text{C}_8\text{H}_{10}\text{O}_4\text{P}^+$), 187 (10, $\text{C}_8\text{H}_{12}\text{O}_3\text{P}^+$), 91 (5, C_7H_7^+), compatible with mass spectrum fragments of phosphorus compounds (Fig. 2).

Figures 3 and 4 show thermogravimetric analysis of organophosphate. According to the results, it is noteworthy that organophosphate exhibits thermal and oxidative stabilities smaller than diphenyl phosphate. Organophosphate shows a T_{onset} of oxidation at $37\text{ }^{\circ}\text{C}$, which is $235\text{ }^{\circ}\text{C}$ lower than diphenylphosphate. This trend suggest that as the ratio of alkyl (alkoxy: $-\text{OC}_2\text{H}_5$)/aryl (phenoxy: $-\text{OC}_6\text{H}_5$) groups increases in the organophosphate molecules, oxidative stability decreases [28]. However, after the first thermal degradation event ($47\text{ }^{\circ}\text{C}$ (N_2) and $37\text{ }^{\circ}\text{C}$ (air)), stable species were formed with degradation temperatures higher than diphenyl phosphate. In previous work, similar behavior was observed in molecules of the same class [27]. The values of IPDT calculated by Doyle's [23] method is in the range of $360\text{--}429\text{ }^{\circ}\text{C}$. The value of IPDT represents an overall thermal stability of the materials. Table 1 summarizes the thermal parameters of organophosphate and diphenyl phosphate.

Fig. 2 GC–MS of organophosphate

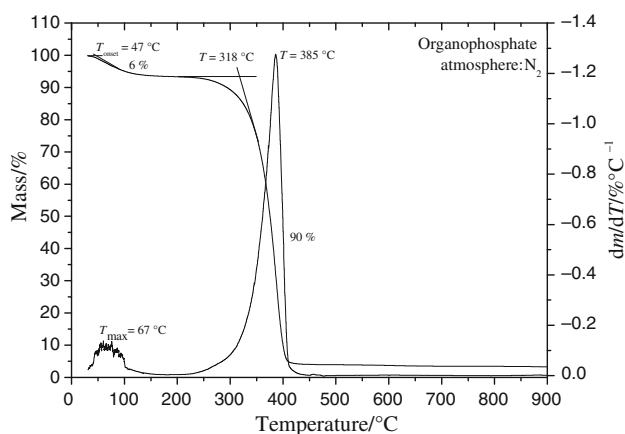
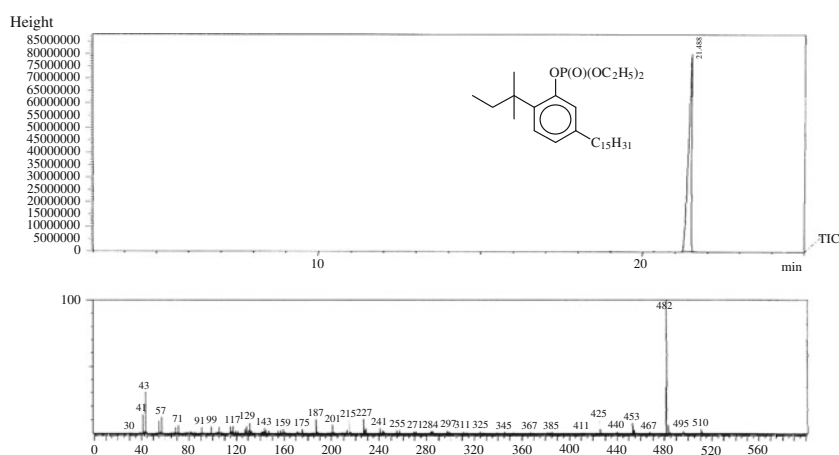


Fig. 3 TG–DTG curves of organophosphate in nitrogen atmosphere

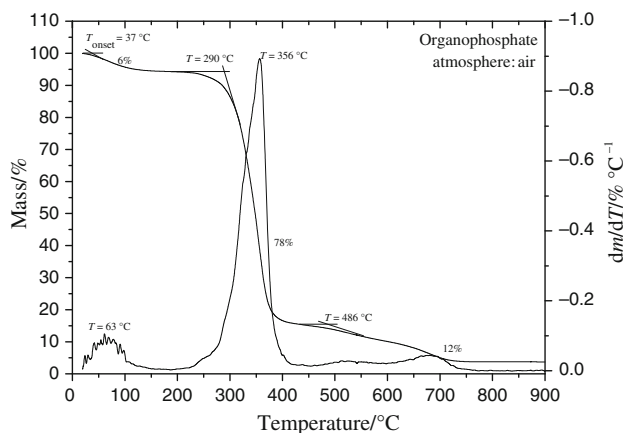


Fig. 4 TG–DTG curves of organophosphate in air atmosphere

Thermal degradation DSC profile of organophosphate is shown in Fig. 5, and data are given in Table 2. From results presented in Table 2, it is apparent that organophosphate shows a good thermal stability, with T_{onset} of degradation at 178 °C for the first peak. This thermal behavior can be related to its basic structure, once that the

aromatic ring and the *tert*-amyl group attached on the aromatic ring present in organophosphate exhibit a great thermal stability [29]. In an inert gas atmosphere, if TG (weight loss) data are seen at a temperature below the T_{onset} of DSC measurements (thermal degradation), it would suggest that this weight loss is due to volatility and not due to thermal degradation. Similarly, weight loss above thermal degradation onset temperature would be a result of degradation along with volatility [29].

As seen in Table 2, DSC profile of organophosphate shows four peaks and the first peak, with onset temperature occurring above weight loss onset temperature (Fig. 3), hence, this weight loss, would be due to volatility alone. As shown in Fig. 5, organophosphate presented four thermal events: one exothermic (first event) and three endothermic (second, third, and fourth events). The first event occurring probably due to polymerization reaction and the others due to thermal degradation [28, 29].

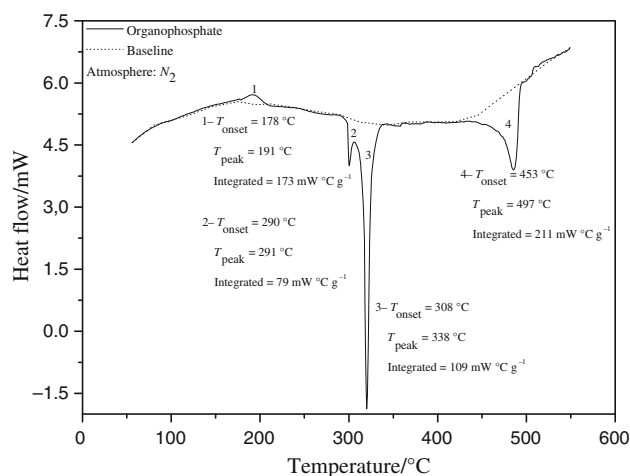
Differential thermal analysis

For evaluation of antioxidant effectiveness of organophosphate comparing results with alkylphenol and diphenyl phosphate was used a thermoanalytical technique—DTA. This technique permits to predict the initial decomposition temperature—IDT, which precedes the main oxidation process. The existence of the reactions occurring during the IDT is not detected by the experimental technique used so that seemingly no reaction takes place. In fact, IDT is a preparatory stage in which the entities needed for the full development of autoxidation are formed. The high IDT is considered a relative measure of the stability of materials [26].

Differential thermal analysis measurements are shown in Figs. 6, 7, 8 and given in Table 3. According to the results, antioxidant effectiveness of organophosphate can be proven by the difference between IDT for mineral oil (91.28 °C) and mineral oil + organophosphate (1%)

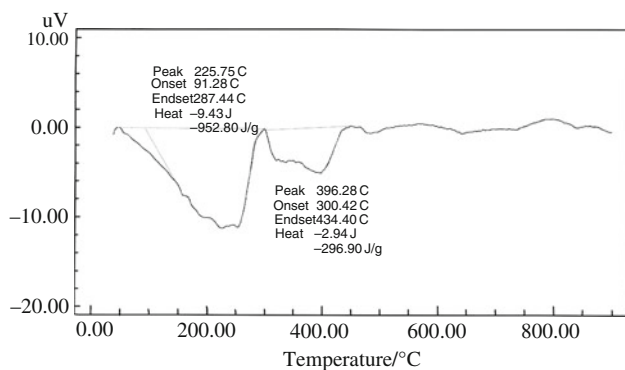
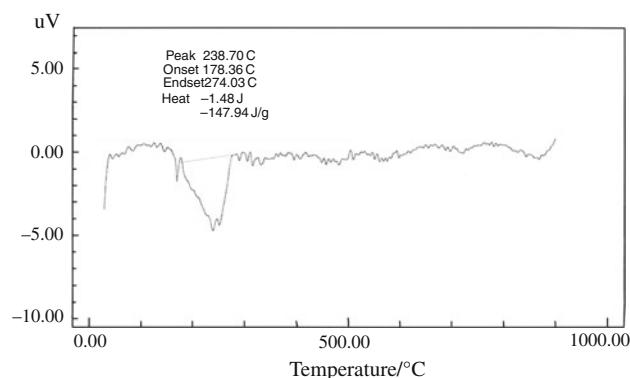
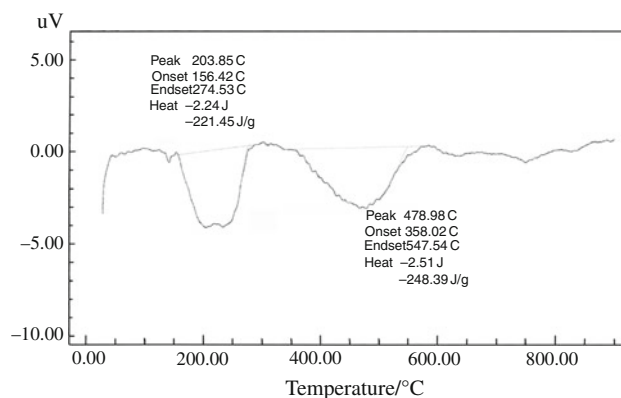
Table 1 Thermal parameters of organophosphate and diphenyl phosphate

Sample	Degradation event		$T_{\text{onset}}/^{\circ}\text{C}$		$T_{\text{max}}/^{\circ}\text{C}$		$\Delta m/\%$		IPDT/ $^{\circ}\text{C}$	
	Air	N ₂	Air	N ₂	Air	N ₂	Air	N ₂	Air	N ₂
Organophosphate	III	II	37 (I)	47 (I)	63 (I)	67 (I)	6 (I)	6 (I)	360	371
			290 (II)	318 (II)	356 (II)	385 (II)	78 (II)	90 (II)		
			486 (III)		680 (III)		12 (III)			
Diphenyl phosphate	III	–	252 (I + II)	–	301 (I)	–	87 (I + II)	–	429	–
			550 (III)		352 (II)					
					604 (III)		3 (III)			

**Fig. 5** DSC curve of organophosphate in nitrogen atmosphere**Table 2** DSC measurements of organophosphate (N₂ atmosphere)

Sample	Thermal transitions	$T_{\text{onset}}/^{\circ}\text{C}$	$T_{\text{peak}}/^{\circ}\text{C}$	Integrated/ $\text{mW } ^{\circ}\text{C g}^{-1}$
Organophosphate	I	178	191	173
	II	290	291	79
	III	308	338	109
	IV	453	497	211

T_{peak} peak temperature, *Integrated* involved energy

**Fig. 6** DTA curve of mineral oil in air atmosphere**Fig. 7** DTA curve of mineral oil + alkylphenol (1%) in air atmosphere**Fig. 8** DTA curve of mineral oil + organophosphate (1%) in air atmosphere

(156.42 °C). This behavior can be explained partly by the substituent presence at the *meta* and/or *ortho* positions. The bulkier substituents such as *tert*-amyl on *ortho*- and/or *para*-positions have been recommended to inhibit coupling reaction of phenoxy radicals, resulting in the decrease of oxidation rate [14, 24]. For example, organophosphate has bulkier substituent on both *ortho* and *meta* positions and, consequently, shows a good thermo-oxidative stability, because this molecule possesses extensively conjugated structure that is efficient in scavenging free radicals. The

Table 3 DTA measurements of mineral oil with and without additives (air atmosphere)

Sample	IDT/°C Air	T_{\max} /°C Air	Heat/J g ⁻¹ °C ⁻¹
Mineral oil	91.28	225.75	-952.80
Mineral oil + alkylphenol (1%)	178.38	238.70	-147.94
Mineral oil + organophosphate (1%)	156.42	203.85	-221.45
Mineral oil + diphenyl phosphate (1%)	152.13	200.50	-82.83

sample mineral oil + alkylphenol (1%) exhibited a considerably result too. In this molecule (alkylphenols), the presence of *ortho* substituent (α -hydrogen) was important for its antioxidant activity.

As seen in Table 3, the peak temperatures (T_{\max}) are in the order of stability: mineral oil + organophosphate (1%) > mineral oil + diphenyl phosphate (1%), proving once again the antioxidant effectiveness of organophosphate. The decrease of energy involved in oxidation processes showed that the oxidation rate of the samples with antioxidant presented lower values [11, 12, 30, 31]. Therefore, the organophosphate derived from biomass (CNSL) presents promising potential for industries that work in consonance with green chemistry.

Conclusions

Results indicated that organophosphate is an efficient antioxidant when compared with a product of the same class (diphenyl phosphate). This behavior can be explained in terms by its chemical structure at once that has bulkier substituent on both *ortho* and *meta* positions and highly stable P–O–C bond. DTA indicate that the thermal stability are in the order: mineral oil + organophosphate (1%) > mineral oil + diphenyl phosphate (1%) proving the antioxidant effectiveness of organophosphate and its TG–DTG curves showed that after the first thermal degradation event (47 °C (N₂) and 37 °C (air)), stable species were formed with degradation temperatures higher than diphenyl phosphate (a commercial product). DSC profile of organophosphate showed that the compound exhibited a good thermal stability, with T_{onset} of degradation at 178 °C for the first peak. This thermal behavior can be related to its basic structure once that the aromatic ring and the *tert*-amyl group attached on the aromatic ring present in organophosphate exhibit a great thermal stability. Therefore, the organophosphate derived from biomass (CNSL) presents promising potential for industries that work in consonance with green chemistry.

Acknowledgements The authors acknowledge Petróleo Brasileiro S.A. (PETROBRAS) and CNPq (Process number 472009/2007-9) for the financial support, the Organic and Inorganic Chemistry Department of Federal University of Ceará by chemical and thermal analyses, and the Northeastern Center of Application and Use of Nuclear Magnetic Resonance—CENAUREM/UFC by ¹H, ¹³C, and ³¹P NMR.

References

- Santos JCO, Santos IMG, Sinfrônio FSM, Silva MA, Sobrinho EV. Thermodynamic and kinetic parameters on thermal degradation of automotive mineral lubricant oils determined using thermogravimetry. *J Therm Anal Calorim.* 2005;79:461–7.
- Castro Dantas TN, Dantas MSG, Dantas Neto AA, D'Ornellas CV, Queiroz LR. Novel antioxidants from cashew nut shell liquid applied to gasoline stabilization. *Fuel.* 2003;82:1465–9.
- Santos JCO, Lima LN, Santos IMG, Souza AG. Thermal, spectroscopic and rheological study of mineral base lubricant oils. *J Therm Anal Calorim.* 2007;87:639–43.
- Sevim ZE, Svajus A. Lubricant basestocks from vegetable oils. *Ind Crop Prod.* 2000;11:277–82.
- Keating MY, Howell JL. Decomposition of perfluoropolyether lubricants. A study using TG-MS in the presence of alumina powder. *J Therm Anal Calorim.* 2011;106:213–20.
- Ren D, Gellman AJ. Reaction mechanisms in organophosphate vapor phase lubrication of metal surfaces. *Tribol Int.* 2001;34:353–65.
- Rizvi SQA. A comprehensive review of lubricant chemistry, technology, selection, and design. ASTM International: EUA; 2008.
- Fox NJ, Stachowiak GW. Vegetable oil-based lubricants—a review of oxidation. *Tribol Int.* 2007;40:1035–46.
- Perez JM. Oxidation studies of lubricants from dornte to microreactors. ASTM STP 1326; 1997.
- Raimundo CRN, Daniel OL, Thauzer DSP, Rômulo FA, Tereza NCD, Michelle SGD, Maria ASA, LC Célio Jr, Diana CSA. Thermo-oxidative stability of mineral naphthenic insulating oils: combined effect of antioxidants and metal passivator. *Ind Eng Chem Res.* 2004;43:7428–34.
- Maria ARF, Selma EM, José OBC, Glaucione GB. Evaluation of antioxidant properties of a phosphorated cadanol compound on mineral oils (NH10 and NH20). *Fuel.* 2007;86:2416–21.
- Maria ARF. Síntese e Aplicabilidade de Antioxidantes derivados do Cardanol hidrogenado. Thesis (Doctor), Organic and Inorganic Chemical Department, Federal University of Ceará, Brazil 2008.
- José Carlos OS, Iêda MGS, Antonio GS, Eledir VS, Valter JF, Arilson JNS. Thermoanalytical and rheological characterization of automotive mineral lubricants after thermal degradation. *Fuel.* 2004;83:2393–9.
- Maria ASR, Francisco AMS, Selma EM. Study of antioxidant properties of 5-*n*-pentadecyl-2-*tert*-amylphenol. *Energy Fuel.* 2009;23:2517–22.
- Francisco HAR, Judith PAF, Nágila MPSR, Francisco CFF, José OBC. Antioxidant activity of cashew nut shell liquid (CNSL) derivatives on the thermal oxidation of synthetic cis-1,4-polyisoprene. *J Braz Chem Soc.* 2006;17:265–71.
- Chaithongdee D, Chutmanop J, Srinophakun P. Effect of antioxidants and additives on the oxidation stability of jatropa biodiesel. *Kasetsart J (Nat Sci).* 2010;44:243–50.
- Rodrigues MGF, Souza AG, Santos IMG, Bicudo TC, Silva MCD. Antioxidative properties of hydrogenated cardanol for cotton biodiesel by PDSC and UV/VIS. *J Therm Anal Calorim.* 2009;97:605–9.

18. Rios MAS, Mazzetto SE. Procedimentos de Preparação de Aditivos Organofosforados obtidos da Modificação Química do 3-*n*-pentadecilfenol para Aplicação nos Setores Industriais. PI0801708-5A2, 2008.
19. Lomonaco D, Cangane FY, Mazzetto SE. Thiophosphate esters of cashew nutshell liquid derivatives as new antioxidants for poly(methyl methacrylate). *J Therm Anal Calorim.* 2011;104:1177–83.
20. Rajesh NP, Santanu B, Anuradda G. Extraction of cashew (*Anacardium occidentale*) nut shell liquid using supercritical carbon dioxide. *Bioresour Technol.* 2006;97:847–53.
21. Kumar PP, Paramashivappa R, Vithayathil PJ, Rao PVS, Rao AS. Process for isolation of cardanol from technical cashew (*Anacardium occidentale* L.) nut shell liquid. *J Agric Food Chem.* 2002;50:4705–8.
22. Paramashivappa R, Kumar PP, Vithayathil PJ, Rao AS. Novel method for isolation of major phenolic constituents from cashew (*Anacardium occidentale* L.) nut shell liquid. *J Agric Food Chem.* 2001;49:2548–51.
23. Doyle CD. Estimating thermal stability of experimental polymers by empirical thermogravimetric analysis. *Anal Chem.* 1961;33:77–9.
24. Rios MAS, Santiago SN, Lopes AAS, Mazzetto SE. Antioxidative activity of 5-*n*-pentadecyl-2-*tert*-butylphenol stabilizers in mineral lubricant oil. *Energy Fuel.* 2010;24:3285–91.
25. Silverstein RM, Webster FX, Kiemle DJ. Spectrometric identification of organic compounds. 7th ed. New York: Wiley; 2005.
26. Wendlandt WW. Thermal methods of analysis. New York: Wiley; 1964.
27. Rios MAS, Nascimento TL, Santiago SN, Mazzetto SE. Cashew nut shell liquid: a versatile raw material utilized for syntheses of phosphorus compounds. *Energy Fuel.* 2009;23:5432–7.
28. Shankwalkar SG, Placek DG. Oxidation and weight loss characteristics of commercial phosphate esters. *Ind Eng Chem Res.* 1992;31:1810–3.
29. Shankwalkar SG, Cruz C. Thermal degradation and weight loss characteristics of commercial phosphate esters. *Ind Eng Chem Res.* 1994;33:740–3.
30. Xiao J, Hu Y, Yang L, Cai Y, Song L, Chen Z, Fan W. Fire retardant synergism between melamine and triphenyl phosphate in poly(butylene terephthalate). *Polym Degrad Stabil.* 2006;91:2093–100.
31. Ortuoste N, Allen NS, Papanastasiou M, McMahon A, Edge M, Johnson B, Keck-Antoine K. Hydrolytic stability and hydrolysis reaction mechanism of bis(2,4-di-*tert*-butyl)pentaerythritol diphosphite (Alkanox P-24). *Polym Degrad Stabil.* 2006;91:195–211.